

Galerkin boundary integral analysis for the axisymmetric Laplace equation^{||}

L. J. Gray^{1,3,*}, Maria Garzon^{2,‡}, Vladislav Mantić^{3,§} and Enrique Graciani^{3,¶}

¹*Computer Science and Mathematics Division, Oak Ridge National Laboratory, Oak Ridge, TN 37831, U.S.A.*

²*Department of Applied Mathematics, University of Oviedo, Oviedo, Spain*

³*Elasticity and Strength of Materials Group, University of Seville, Camino de los Descubrimientos, s/n, 41092 Seville, Spain*

SUMMARY

The boundary integral equation for the axisymmetric Laplace equation is solved by employing modified Galerkin weight functions. The alternative weights smooth out the singularity of the Green's function at the symmetry axis, and restore symmetry to the formulation. As a consequence, special treatment of the axis equations is avoided, and a symmetric-Galerkin formulation would be possible. For the singular integration, the integrals containing a logarithmic singularity are converted to a non-singular form and evaluated partially analytically and partially numerically. The modified weight functions, together with a boundary limit definition, also result in a simple algorithm for the post-processing of the surface gradient. Published in 2005 by John Wiley & Sons, Ltd.

KEY WORDS: axisymmetric Laplace; boundary integral equation; Galerkin approximation; singular integration

*Correspondence to: L. J. Gray, Computer Science and Mathematics Division, ORNL, Oak Ridge, TN 37831, U.S.A.

†E-mail: ljpg@ornl.gov, graylj1@ornl.gov

‡E-mail: maria@orion.ciencias.uniovi.es

§E-mail: mantic@esi.us.es

¶E-mail: graciani@esi.us.es

^{||}This article is a U.S. Government work and is in the public domain in the U.S.A.

Contract/grant sponsor: Spanish Ministry of Education, Culture and Sport; contract/grant number: SAB 2003-0088

Contract/grant sponsor: Spanish Ministry of Science and Technology; contract/grant numbers: MAT 2003-03315, MEC-04-MTM-05417

Contract/grant sponsor: U.S. Department of Energy; contract/grant number: DE-AC05-00OR22725

Received 15 July 2005

Revised 31 October 2005

Accepted 9 November 2005

1. INTRODUCTION

This paper presents a Galerkin boundary integral implementation for the three-dimensional axisymmetric Laplace equation. Beginning in the mid-1970s [1–3], collocation solutions of integral equations for axisymmetric problems have been extensively considered in the literature [4]. Recent work has focused on axisymmetric elasticity [5–8], in particular for fracture and contact analysis. Although the Galerkin approach has probably been applied to solve axisymmetric boundary integral equations, we have been unable to locate any papers on this subject.

One key aspect in a boundary integral formulation for an axisymmetric problem is that the Green's function has a different singular behaviour when the source point is on the symmetry axis. For a point off the axis, the Green's function represents (rotating around the symmetry axis), a ring source in three dimensions. However, for a point on the axis, the ring source degenerates to a single point, and thus some difference in behaviour is to be expected.

The consequences for a collocation approximation are significant. In a standard collocation analysis, an equation is written with the source point on the symmetry axis, and thus the singular integration for this equation is necessarily different from that in other equations. This adds an additional complication to the analysis, and a variety of techniques have been employed, including the use of a different fundamental solution on the axis (see Reference [7] and references therein). While having to work with a second Green's function clearly involves additional work when implementing the method, this axis solution is, on the other hand, a simpler function than the general expression.

One of the goals of the present work is to demonstrate that, by using a Galerkin technique, no special treatment is required at the axis. This comes about partly due to the weak formulation, as no equation is written 'directly' at the axis, and partly due to the use of modified Galerkin weighting functions. The weight functions employed herein are in fact zero at the axis, which effectively counterbalances the different behaviour of the Green's functions at the axis. This greatly simplifies the on-axis singular integration analysis, for both first- and second-order derivatives of the Green's function. Moreover, an additional important benefit of the modified weight functions is that they restore symmetry to the formulation, permitting a symmetric-Galerkin formulation [9].

The axisymmetric Green's functions, given in terms of complete elliptic integrals, also differ from their standard two-dimensional counterparts in that there is a logarithm singularity in all kernel functions. This integrable singularity obviously requires an appropriate numerical treatment, and this is impeded by the complicated form of these weakly singular terms. A second aim of this work is to propose a hybrid analytic/numeric method for the evaluation of these singular integrals. The method is based upon reformulating the integral as a non-singular double integral, as in Reference [10], and then evaluating one part of the integral analytically.

Our primary motivation in pursuing this work was to solve moving boundary problems, and in these simulations the surface gradient of the potential is the quantity of interest. A standard boundary integral representation of the gradient involves second-order derivatives of the Green's function, and moreover requires a complete integration over the boundary (see Reference [11] for a discussion of boundary integral gradient evaluation methods). Herein we show that the boundary limit approach in References [12, 13] is advantageous, in that all of the complexity of the axisymmetric kernel functions disappears: the kernels for gradient evaluation are no more difficult than for the simple two-dimensional Laplace equation. Moreover, the complete boundary integration can be reduced to considering only the coincident singular integration.

We focus on the analysis of the integral equation for surface potential ϕ , $\nabla^2\phi=0$. However, we expect that these techniques will apply directly to the hypersingular equation for surface flux, and moreover, to the much more complicated axisymmetric formulation for elasticity [4, 6–8, 14].

2. AXISYMMETRIC FORMULATION

The derivation of the boundary integral formulation for the three-dimensional axisymmetric Laplace equation can be found in many books, e.g. References [15, 16], the presentation herein follows the notation in Reference [17]. The basic procedure is to start with the standard boundary integral equation for surface potential [16, 18], replace the Cartesian co-ordinates (x, y, z) with cylindrical co-ordinates (r, θ, z) , and integrate with respect to θ . As the boundary potential and flux are independent of θ , the interior and exterior integral equations for the potential take the form

$$\begin{aligned}\phi(\hat{r}, \hat{z}) &= \int_{\Gamma} r \left(\frac{\partial\phi}{\partial\mathbf{n}}(r, z)G(\hat{r}, \hat{z}; r, z) - \phi(r, z)\frac{\partial G}{\partial\mathbf{n}}(\hat{r}, \hat{z}; r, z) \right) d\Gamma_{rz} \\ 0 &= \int_{\Gamma} r \left(\frac{\partial\phi}{\partial\mathbf{n}}(r, z)G(\hat{r}, \hat{z}; r, z) - \phi(r, z)\frac{\partial G}{\partial\mathbf{n}}(\hat{r}, \hat{z}; r, z) \right) d\Gamma_{rz}\end{aligned}\quad (1)$$

the Green's function kernels to be defined below. In the first equation, (\hat{r}, \hat{z}) is a point *interior* to the domain, and in the second (\hat{r}, \hat{z}) lies outside. These equations are also valid for $(\hat{r}, \hat{z}) \in \Gamma_{rz}$, and are in fact then identical, with an appropriate definition of the singular integrals [19]. The line integral is with respect to the point (r, z) (subsequently the subscript on Γ will be omitted), and the boundary contour Γ is the $x > 0$ section of the intersection of the three-dimensional boundary surface with the $y=0$ plane. For what is to follow, it is worth noting that the θ integral is over a circle of radius r , and thus the r factor in Equation (1) comes from the Jacobian of this integration.

The axisymmetric Green's function $G(\hat{r}, \hat{z}; r, z)$ and its normal derivative are defined in terms of the complete elliptic integrals of the first and second kind, $K(m)$ and $E(m)$

$$G(\hat{r}, \hat{z}; r, z) = \frac{1}{\pi} \frac{1}{(a+b)^{1/2}} K(m) \quad (2)$$

$$\frac{\partial G}{\partial\mathbf{n}}(\hat{r}, \hat{z}; r, z) = \frac{1}{\pi} \left[\frac{n_r}{2r(a+b)^{1/2}} \{E(m) - K(m)\} - \frac{\mathbf{n} \cdot \mathbf{R}}{(a-b)(a+b)^{1/2}} E(m) \right] \quad (3)$$

Here $a = r^2 + \hat{r}^2 + \Delta z^2$, $b = 2r\hat{r}$, $\Delta r = r - \hat{r}$, $\Delta z = z - \hat{z}$, $\mathbf{R} = (\Delta r, \Delta z)$ and $\mathbf{n} = \mathbf{n}(r, z)$ is the unit outward normal at the field point. Adopting the notation in Reference [20]

$$\begin{aligned}K(m) &= \int_0^{\pi/2} \frac{d\theta}{(1 - m \sin^2(\theta))^{1/2}} \\ E(m) &= \int_0^{\pi/2} (1 - m \sin^2(\theta))^{1/2} d\theta\end{aligned}\quad (4)$$

where the parameter m and its complementary parameter $m_1 = 1 - m$ are defined by

$$m = \frac{2b}{a+b} = \frac{4r\hat{r}}{(r+\hat{r})^2 + \Delta z^2} \tag{5}$$

$$m_1 = \frac{a-b}{a+b} = \frac{\Delta r^2 + \Delta z^2}{(r+\hat{r})^2 + \Delta z^2}$$

The formula for the normal derivative of G can be derived by using the relations [21]

$$\frac{d}{dk} \tilde{K}(k) = \frac{\tilde{E}(k)}{k(1-k^2)} - \frac{\tilde{K}}{k} \tag{6}$$

$$\frac{d}{dk} \tilde{E}(k) = \frac{\tilde{E}(k) - \tilde{K}(k)}{k}$$

where $\tilde{K}(k) = K(k^2)$ and $\tilde{E}(k) = E(k^2)$.

To evaluate $E(m)$ and $K(m)$, we will use the polynomial approximations developed by Hastings [22]

$$K(m) \approx \sum_{v=0}^4 a_v m_1^v - \log(m_1) \sum_{v=0}^4 b_v m_1^v \tag{7}$$

$$E(m) \approx 1 + \sum_{v=1}^4 c_v m_1^v - \log(m_1) \sum_{v=1}^4 d_v m_1^v$$

the error in these expansions being less than 2×10^{-8} ; the coefficients $\{a_v, b_v, c_v, d_v\}$ can be found in Reference [20]. Thus, as expected, G has a logarithmic singularity for $(\hat{r}, \hat{z}) \rightarrow (r, z)$ ($m_1 = 1 - m = 0$), and its normal derivative behaves as $\|(\Delta r, \Delta z)\|^{-1}$. The logarithmic singularity is, however, also present in the normal derivative of G , and thus the numerical treatment of this integral will also have to take into account the presence of this integrable singularity.

Moreover, as noted in Section 1, the singular behaviour is different at the symmetry axis. Note that $a + b$ appears in the denominator in Equation (2) and Equation (3), and $a + b = r^2 + \hat{r}^2 + \Delta z^2 = 0$ when $r = \hat{r} = \Delta z = 0$. In this regard, a Galerkin approximation has an immediate advantage, in that unlike collocation, an equation is not written precisely at the axis. Moreover, the standard Galerkin weight functions will be modified, and this will eliminate any difficulties in handling this axis singularity. This will be the case not only for the equation for surface potential, but also for the (hypersingular) derivative equation for surface flux.

2.1. Galerkin approximation

In the following, the singular integrals will be defined as a limit to the boundary [19], and to simplify the notation, we employ $Q = (r, z)$ and $P = (\hat{r}, \hat{z})$. For convenience, the *exterior limit* form of Equation (1) will be employed, and can be written as

$$\mathcal{P}(P) \equiv \lim_{\varepsilon \rightarrow 0^+} \int_{\Gamma} r \left(\frac{\partial \phi}{\partial \mathbf{n}}(Q) G(P_\varepsilon, Q) - \phi(Q) \frac{\partial G}{\partial \mathbf{n}}(P_\varepsilon, Q) \right) d\Gamma_Q = 0 \tag{8}$$

where $P_\varepsilon = (\hat{r}_\varepsilon, \hat{z}_\varepsilon) = (\hat{r}, \hat{z}) + \varepsilon \mathbf{N}$, $\mathbf{N} = \mathbf{N}(P)$ being the unit outward normal at $P = (\hat{r}, \hat{z})$.

The two somewhat irritating aspects of this axisymmetric boundary integral equation were alluded to in Section 1. First, although $G(P, Q) = G(Q, P)$ is, as expected, a symmetric function of field and source points, rG is clearly not, and the matrix resulting from this integral will not be symmetric if the usual Galerkin procedure is applied. Second, as previously noted, the kernel functions contain an additional singularity at the axis $r = \hat{r} = 0$, due to the presence of the $a + b$ term in the denominators. This singularity causes some difficulty for collocation approximations, and the same would be true here if, once again, standard Galerkin weight functions were employed. Fortunately there is leeway in the choice of the weight functions, and this flexibility will be exploited herein.

In Galerkin, Equation (8) is enforced ‘on average’ by employing a second boundary integration with respect to P

$$0 = \int_{\Gamma} \hat{\psi}_k(P) \mathcal{P}(P) d\Gamma_P \quad (9)$$

The Galerkin weight function $\hat{\psi}_k(P)$ is *usually* composed of all shape functions $\psi_l(P)$ that are non-zero at a particular node P_k ; in particular, this implies $\hat{\psi}_k(P_k) = 1$. To be more specific, in this work we employ a linear interpolation, in which case a segment (element) of the boundary is defined by two nodes, $\{P_0, P_1\}$ and the two linear shape functions on this element are

$$\begin{aligned} \psi_1(t) &= 1 - t \\ \psi_2(t) &= t \end{aligned} \quad (10)$$

where $t \in [0, 1]$ is the parametric variable of the element. In terms of these shape functions, the basic approximations of the boundary and boundary functions are then

$$\begin{aligned} Q(s) &= \psi_1(s)P_0 + \psi_2(s)P_1 \\ \phi(Q(s)) &= \phi(P_0)\psi_1(s) + \phi(P_1)\psi_2(s) \\ \frac{\partial \phi}{\partial \mathbf{n}}(Q(s)) &= \frac{\partial \phi}{\partial \mathbf{n}}(P_0)\psi_1(s) + \frac{\partial \phi}{\partial \mathbf{n}}(P_1)\psi_2(s) \end{aligned} \quad (11)$$

To regain the symmetry (thereby allowing a symmetric-Galerkin formulation), and to ameliorate the axis singularity, the obvious course of action is to take the standard weight functions $\hat{\psi}_k(P)$ and multiply by \hat{r} . Thus, the equations to be solved take the form

$$0 = \lim_{\varepsilon \rightarrow 0^+} \int_{\Gamma} \hat{r} \hat{\psi}_k(P) \int_{\Gamma} r \left(\frac{\partial \phi}{\partial \mathbf{n}}(Q) G(P_\varepsilon, Q) - \phi(Q) \frac{\partial G}{\partial \mathbf{n}}(P_\varepsilon, Q) \right) d\Gamma_Q d\Gamma_P \quad (12)$$

Moreover, the equation for surface flux is

$$0 = \lim_{\varepsilon \rightarrow 0^+} \int_{\Gamma} \hat{r} \hat{\psi}_k(P) \int_{\Gamma} r \left(\frac{\partial \phi}{\partial \mathbf{n}}(Q) \frac{\partial G}{\partial \mathbf{N}}(P_\varepsilon, Q) - \phi(Q) \frac{\partial^2 G}{\partial \mathbf{n} \partial \mathbf{N}}(P_\varepsilon, Q) \right) d\Gamma_Q d\Gamma_P \quad (13)$$

where derivatives with respect to $\mathbf{N}(P)$ are with respect to $P = (\hat{r}, \hat{z})$. With the additional factor of \hat{r} , these equations possess the same symmetry properties as standard boundary integral formulations [9], and a symmetric-Galerkin formulation is possible.

The concern in modifying the weight functions in this manner is that now *all* weight functions are zero at the axis, possibly wiping out information needed to solve for the axis unknowns (i.e. it is possible that an ill-conditioned systems of equations might result). A plausible explanation for why this does not happen is that non-axis points represent a ring source, whereas an axis point is a degenerate single point; thus, assigning a weight of 0 to the equation precisely at this point is physically reasonable, and turns out to be computationally sound. In fact this approach corresponds to starting with a 3-D Galerkin boundary integral formulation, and then, as in the derivation of Equation (1), integrating out the angular variable in the cylindrical representation of P . The Jacobian of the cylindrical co-ordinates would produce an \hat{r} factor in the boundary integral, as in the above equations.

Moreover, as there is no extra difficulty on the axis in the fully three-dimensional formulation, it is not surprising that the \hat{r} factor helps to mollify the kernel function behaviour on the axis. As will be seen below in the gradient discussion, this is especially useful for treating the derivative of Equation (8) (e.g. hypersingular equation for surface flux). We note that a similar approach has been taken in a weak formulation of contact conditions in axisymmetric elasticity [7] using a collocational BEM.

3. SINGULAR INTEGRATION

For the most part, the boundary limit evaluation of the singular integrals follows the procedures described in Reference [19]. In particular, the most singular part of $\partial G/\partial \mathbf{n}$, comes solely from the last term in Equation (3)

$$\frac{\mathbf{n} \cdot \mathbf{R}}{(a-b)(a+b)^{1/2}} E(m) \quad (14)$$

and moreover only from $E(1)=1$. For the coincident Galerkin integral, $(a+b)^{1/2}$ can be replaced by $2\hat{r}$, and with these substitutions the above function is then essentially the same as the first derivative kernel for two-dimensional Laplace equation. There is therefore no difficulty in the analytic evaluation of the integral and the boundary limit. Herein we therefore focus on the one major new aspect present in the axisymmetric analysis: there is now, in both kernel functions, a logarithmic singularity having a fairly complicated coefficient. While integrable, these logarithm terms cannot be accurately evaluated with standard Gauss quadrature. Although the specialized Gauss rules for a log singularity [23] could be employed, we have opted to extend the analytic integration procedures as far as possible.

The troublesome $\log(m_1)$ expression is

$$\log\left(\frac{a-b}{a+b}\right) = \log(\Delta r^2 + \Delta z^2) - \log((r + \hat{r})^2 + \Delta z^2) \quad (15)$$

and it is the first term on the right that is the primary concern. We first show that for both coincident and adjacent singular integrals, the log integrals take the form

$$\int_0^\beta \mathcal{F}(x) \log(Ax) dx \quad (16)$$

where A is a constant with respect to x , but may be a function of other variables (Equation (16) being just one part of a multidimensional integral). A possible approach would be

to write

$$\int_0^\beta \mathcal{F}(x) \log(Ax) dx = \beta \log(A\beta) \int_0^1 \mathcal{F}(\beta z) dz + \beta \int_0^1 \mathcal{F}(\beta z) \log(z) dz \quad (17)$$

thereby removing the constant A and allowing the log singularity to be handled by specialized Gauss rules. However, as this would require a separate numerical integration of the first term on the right, we have chosen to treat the entire integral in Equation (16), employing analytic integration as much as possible.

The function $\mathcal{F}(x)$ arising from the axisymmetric kernels is sufficiently complicated that analytic integration is not possible. Again a possible algorithm would be to use a Taylor series (at $x=0$) for \mathcal{F} , integrating the polynomial part analytically and the remainder numerically [24]. However, given the complexity of the logarithm functions for axisymmetric analysis (in particular, considering future applications in elasticity), this would be fairly tedious to implement for the potential equation, and much worse in implementing the equation for surface flux. Moreover, for higher order interpolation, the Jacobians are not constants, and this would complicate matters even further. We have therefore implemented a numerical treatment based upon extending the procedure in Reference [10] designed to handle the simple case $A=\beta=1$.

We first briefly demonstrate that, Equation (14) aside, the remaining singular integrations reduce to integrals of the form Equation (16), further details can be found in Reference [19]. The two types of Galerkin singular integrals, coincident and adjacent, are discussed separately.

3.1. Adjacent integration

Assume that the adjacent elements are $E_Q = (P_1, P_2)$ and $E_P = (P_2, P_3)$, the reverse situation (E_P precedes E_Q) can be handled similarly. If s and t denote the parameters for the Q and P integrations, respectively, the singularity $Q = P = P_2$ is at $1-s=0$, $t=0$. By introducing polar co-ordinates $\{\rho, \vartheta\}$

$$t = \rho \cos(\vartheta), \quad 1-s = \rho \sin(\vartheta) \quad (18)$$

the singularity is then identified by $\rho=0$, and $\Delta r^2 + \Delta z^2 = \alpha^2 \rho^2$, α being a function of ϑ . Thus, the integration of the logarithm term $\log(\Delta r^2 + \Delta z^2) = 2 \log(\alpha\rho)$ takes the form given in Equation (16)

$$2 \int_0^{\pi/4} d\vartheta \int_0^{1/\cos(\vartheta)} \rho f(\rho, \vartheta) \log(\alpha\rho) d\rho + 2 \int_{\pi/4}^{\pi/2} d\vartheta \int_0^{1/\sin(\vartheta)} \rho f(\rho, \vartheta) \log(\alpha\rho) d\rho \quad (19)$$

3.2. Coincident integration

For the coincident integration, $E_P = E_Q = E$, and the integral is singular when $s=t$. Replacing s by the variable w , $s=w+t$, the coincident integral is

$$\begin{aligned} & 2 \int_0^1 dt \int_{-t}^{1-t} f(w) \log(\alpha|w|) dw \\ & = 2 \int_0^1 dt \int_0^{1-t} f(w) \log(\alpha w) dw + 2 \int_0^1 dt \int_0^t f(-w) \log(\alpha w) dw \end{aligned} \quad (20)$$

These integrals are also of the form in Equation (16).

3.3. Axis singularity

In addition to differences in the kernels' algebraic singularities due to $(a + b)^{-1}$ appearing in Equations (2) and (3), and additional logarithmic singularity is present on the axis, the last term in Equation (15). Thus the coincident integration of an axis element contains this additional weak singularity (this is the only part of the calculation for which an axis element is treated differently from other elements). However, the procedure for handling this $\log(a + b)$ term when $E_P = E_Q$ is the same as for the adjacent singular integration. For this term, arrange the parameters so that the node on the axis corresponds to $s = t = 0$, and proceed as in the adjacent case: introduce polar co-ordinates $t = \rho \cos(\vartheta)$, $s = \rho \sin(\vartheta)$. This leads to $a + b = \alpha_+^2 \rho^2$ and $a - b = \alpha_- \rho^2$ and thus $m_1 = \alpha_- / \alpha_+$, independent of ρ . Incorporating the shape functions, the ρ integrals in this case take the simple form $\rho^j \log(\alpha_+ \rho)$, and can be computed analytically. This leaves just the ϑ integration to be evaluated numerically.

3.4. Log integral transformation

As shown above, the singular integration of the complete elliptic integrals requires evaluating integrals of the form Equation (16). The basic idea is to transform these singular integrals into a double integral involving just the non-singular function \mathcal{F} ; the price that is paid for the overall simplicity of this approach is the computational effort required to evaluate the double integrals.

After transforming to the double integral, the expectation is that one could use low order Gauss quadrature for this evaluation. However, numerical tests have shown that the function \mathcal{F} in the coincident integral varies sufficiently rapidly that a large number of Gauss points are required to obtain a converged value of the integral (and thus the same would be true for a log-Gauss quadrature). We will therefore, in the coincident case, integrate one part of the double integral analytically. This makes the implementation somewhat more involved, but on the other hand, reduces the computational work.

To accomplish the transformation of Equation (16), we first assume $A\beta < 1$. The case $A\beta > 1$ (which does not occur in the coincident integration, but may occur in the adjacent) is handled similarly. We have

$$\begin{aligned} \int_0^\beta \mathcal{F}(x) \log(Ax) dx &= \frac{1}{A} \int_0^{A\beta} \mathcal{F}(y/A) \log(y) dy = \frac{1}{A} \int_0^{A\beta} \mathcal{F}(y/A) \int_1^y \frac{1}{u} du dy \\ &= -\frac{1}{A} \int_0^{A\beta} \int_0^u \mathcal{F}(y/A) \frac{1}{u} dy du - \frac{1}{A} \int_{A\beta}^1 \int_0^{A\beta} \mathcal{F}(y/A) \frac{1}{u} dy du \\ &= -\int_0^{A\beta} \int_0^{1/A} \mathcal{F}(uz) dz du - \int_{A\beta}^1 \int_0^{\beta/u} \mathcal{F}(uz) dz du \end{aligned} \tag{21}$$

the last line coming from the change of variables $z = y/(Au)$. The interchange of the order of integrals is illustrated in Figure 1(a). The corresponding result for $A\beta > 1$ is

$$\int_0^\beta \mathcal{F}(x) \log(Ax) dx = -\int_0^1 \int_0^{1/A} \mathcal{F}(uz) dz du + \int_1^{A\beta} \int_{1/A}^{\beta/u} \mathcal{F}(uz) dz du \tag{22}$$

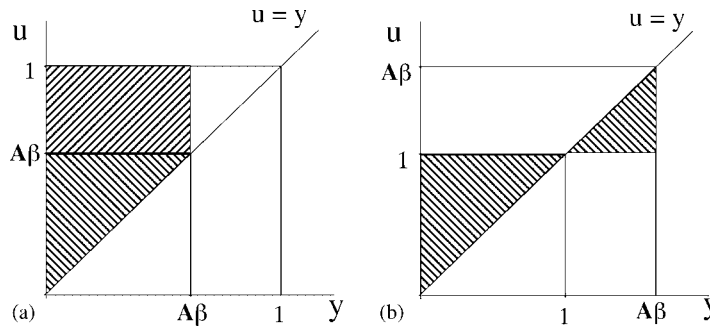


Figure 1. The domains for changing the order of integration in the logarithm integrals.

and the geometry in this case is shown in Figure 1(b). For the simple case $A = \beta = 1$ there is only one double integral, so the minor additional complications are the two integrals, and the two cases depending upon the value of $A\beta$.

3.4.1. Analytic integration: coincident. For the logarithm integrals stemming from the coincident integration, it is necessary to proceed further: numerical evaluation of the double integral using Gauss quadrature turns out to be ineffective. The function \mathcal{F} , the coefficient of the logarithm, is a polynomial in $m_1 = (a - b)/(a + b)$, and this becomes a rational function of the integration variable. For the coincident integral, $a - b = c^2 w^2$ and $a + b = c^2 w^2 + bw + a$, where $w = s - t$. Thus, the function \mathcal{F} for the flux integral is

$$(\psi_{j,0} + w\psi_{j,1}) \frac{\alpha + \beta w}{(w^2 + bw + a)^{1/2}} \sum_{v=0}^4 b_v \left(\frac{w^2}{w^2 + bw + a} \right)^v \quad (23)$$

where $r = \alpha + \beta w$ and $\psi_{j,0} + w\psi_{j,1}$ is the shape function $\psi_j(Q)$ expressed as a polynomial in w . The potential integral lacks this r coefficient, but on the other hand, involves both $E(m)$ and $K(m)$, and is therefore

$$\frac{\psi_{j,0} + w\psi_{j,1}}{(w^2 + bw + a)^{1/2}} \sum_{v=0}^4 (d_v - b_v) \left(\frac{w^2}{w^2 + bw + a} \right)^v \quad (24)$$

Using the procedures of the previous section, w is replaced by uz for the double integral over u and z ; this changes the coefficients, but leaves the form of the rational function unaltered, e.g.

$$\left(\frac{u^2 z^2}{u^2 z^2 + buz + a} \right)^v = \left(\frac{z^2}{z^2 + b'z + a'} \right)^v \quad (25)$$

which has the same form as the w expression, only now $b' = b/u$ and $a' = a/u^2$. These rational functions, together with the appropriate function outside the summations in Equations (23) and (24), can be integrated analytically with respect to z .

Similar expressions can be obtained, in terms of the variable ρ , for the adjacent integration. However, in these cases, analytic integration is less imperative, as the singularity is only at one

point in the double integral. Moreover, note that the polar co-ordinate transformation combines the P and Q integration, and thus both $\hat{r}(P)$ and $\psi_k(P)$ must be incorporated when integrating ρ ; the required analytic expressions are therefore much longer, and the computational advantage of eliminating a numerical integration may in fact disappear. Finally, numerical experiments indicate that the double integral can be accurately evaluated with a low number of Gauss points. As the analytic approach for these integrals appears to have no advantages, and actually some increased complexity in implementation, these integrals have been computed entirely numerically using Equations (21) and (22).

3.5. Analytic integration formulas

A minor difficulty in implementing the analytic integration of the rational functions is that the simplest formulas (provided, say, by integration tables or Maple) breakdown at $\alpha^2 = 4a - b^2 = 0$. This in fact occurs when the element is horizontal, $z(1) = z(2)$. However, it is a simple matter to derive formulas that are valid for all α .

First note that by applying an appropriate change of variables, the required integrals are linear combinations of the simpler integrals of the form

$$\int \frac{Z^j}{(Z^2 + \alpha^2)^{k+1/2}} dZ \quad (26)$$

where $0 < k < 4$ and $0 < j < 2k + 2$. The values of $j > 2k$ are necessary to incorporate the additional w factors in r and $\psi_j(Q)$. Here $\alpha^2 = a - b^2/4 \geq 0$, and for various values of $\{k, j\}$, the simplest analytic expressions contain α in their denominators. For example, when $k = 2$ and $j = 0$

$$\int \frac{1}{(Z^2 + \alpha^2)^{5/2}} dZ = \frac{Z(3\alpha^2 + 2Z^2)}{3\alpha^4(Z^2 + \alpha^2)^{3/2}} \quad (27)$$

which diverges at $\alpha = 0$. However, it is possible to add a constant to this indefinite integral, and subtracting off the coefficient of the $Z^3/(Z^2 + \alpha^2)^{3/2}$ term (the limiting value as $Z \rightarrow \infty$), namely $2/(3\alpha^4)$, results in

$$\frac{3Z\alpha^2 + 2Z^3 - 2(Z^2 + \alpha^2)^{3/2}}{3(Z^2 + \alpha^2)^{3/2}\alpha^4} \quad (28)$$

The final result, clearly well behaved at $\alpha = 0$

$$\int \frac{1}{(Z^2 + \alpha^2)^{5/2}} dZ = - \frac{3Z^2 + 4\alpha^2}{3(Z^2 + \alpha^2)^{3/2}(3Z\alpha^2 + 2Z^3 + 2(Z^2 + \alpha^2)^{3/2})} \quad (29)$$

is now just a matter of rationalizing the numerator. Formulas for all of the integrals that require modification can be found in Appendix.

4. GRADIENT EVALUATION

The post-processing of the complete surface gradient (or stress tensor in elasticity) is important for many applications, and a wide variety of methods have been developed. The literature is

substantial, see for example References [11, 25–29]. The approach employed herein [12, 13] exploits the definition of the integral equations as boundary limits, and therefore falls into the class of methods based upon boundary integral representations. However, as discussed previously [13] and also elaborated on below, this method only requires *local* integrations (as opposed to a complete boundary integral), and therefore has features in common with local averaging methods [30, 31].

More specifically, by taking the difference of the interior and exterior limit integral equations for the gradient, two important simplifications result. The first is that the computational work is drastically reduced: the double Galerkin integration over the complete boundary is replaced by just the singular integrations. In fact, as demonstrated below, the calculation can be reduced to solely the consideration of the coincident integration. Second, the only non-zero contributions are obviously from terms that are ‘discontinuous’ crossing the boundary, and the implications of this for axisymmetric analysis, are substantial. The elliptic integrals, $K(m)$ and $E(m)$, and most especially their log singular terms that required so much attention in solving the potential equation, do not appear at all in the gradient evaluation. The elliptic integrals appear solely through $E(1)=1$, and as a consequence, the integrations can be carried out entirely analytically.

4.1. Gradient equations

The surface gradient equations are obtained by differentiating, with respect to \hat{r} and \hat{z} , the interior and exterior limit potential equations, Equation (1), resulting in

$$\frac{\partial}{\partial \mathcal{X}} \phi(P) = \lim_{\varepsilon \rightarrow 0^-} \int_{\Gamma} r \left(\frac{\partial \phi}{\partial \mathbf{n}}(Q) \frac{\partial G}{\partial \mathcal{X}}(P_{\varepsilon}, Q) - \phi(Q) \frac{\partial^2 G}{\partial \mathcal{X} \partial \mathbf{n}}(P_{\varepsilon}, Q) \right) d\Gamma_Q \quad (30)$$

$$0 = \lim_{\varepsilon \rightarrow 0^+} \int_{\Gamma} r \left(\frac{\partial \phi}{\partial \mathbf{n}}(Q) \frac{\partial G}{\partial \mathcal{X}}(P_{\varepsilon}, Q) - \phi(Q) \frac{\partial^2 G}{\partial \mathcal{X} \partial \mathbf{n}}(P_{\varepsilon}, Q) \right) d\Gamma_Q \quad (31)$$

where \mathcal{X} is either \hat{r} or \hat{z} . Expressions for the kernel functions can be obtained by using Equation (6), and are given by

$$\frac{\partial G}{\partial \hat{r}} = \frac{1}{\pi} \frac{1}{2\hat{r}(a+b)^{1/2}} \left[\frac{r^2 - \hat{r}^2 + \Delta z^2}{a-b} E(m) - K(m) \right] \quad (32)$$

$$\frac{\partial G}{\partial \hat{z}} = \frac{1}{\pi} \frac{\Delta z}{(a-b)(a+b)^{1/2}} E(m)$$

$$\begin{aligned} \frac{\partial^2 G}{\partial \mathcal{X} \partial \mathbf{n}} = & \frac{1}{\pi} \left[\left(\frac{n_r}{2r} - \frac{\mathbf{n} \cdot \mathbf{R}}{a-b} \right) \frac{\partial}{\partial \mathcal{X}} \frac{E(m)}{(a+b)^{1/2}} - \frac{n_r}{2r} \frac{\partial}{\partial \mathcal{X}} \frac{K(m)}{(a+b)^{1/2}} \right. \\ & \left. + \left(\frac{n_{\mathcal{X}}}{a-b} - \frac{\mathbf{n} \cdot \mathbf{R} \Delta \mathcal{X}}{(a-b)^2} \right) \frac{E(m)}{(a+b)^{1/2}} \right] \quad (33) \end{aligned}$$

and

$$\begin{aligned} \frac{\partial}{\partial \mathcal{X}} \frac{K(m)}{(a+b)^{1/2}} &= \pi \frac{\partial G}{\partial \mathcal{X}} \\ \frac{\partial}{\partial \hat{r}} \frac{E(m)}{(a+b)^{1/2}} &= \frac{1}{2\hat{r}(a+b)^{3/2}} \left[(\Delta r^2 - 4\hat{r}^2 + \Delta z^2)E(m) - (r^2 - \hat{r}^2 + \Delta z^2)K(m) \right] \\ \frac{\partial}{\partial \hat{z}} \frac{E(m)}{(a+b)^{1/2}} &= \frac{\Delta z}{(a+b)^{3/2}} [2E(m) - K(m)] \end{aligned} \quad (34)$$

Unlike the two equations for surface potential, for which interior and exterior limits yield the same boundary equation, the two gradient equations are distinct. As in Reference [13], this fact can be exploited by subtracting Equation (31) from (30). In Galerkin form, once again employing the modified weight functions, this ‘limit-difference’ equation takes the form

$$\begin{aligned} \int_{\Gamma} \hat{r} \hat{\psi}_k(P) \frac{\partial}{\partial \mathcal{X}} \phi(P) d\Gamma &= \left\{ \lim_{\varepsilon \rightarrow 0^-} - \lim_{\varepsilon \rightarrow 0^+} \right\} \\ &\times \int_{\Gamma} \hat{r} \hat{\psi}_k \int_{\Gamma} r \left(\frac{\partial \phi}{\partial \mathbf{n}}(Q) \frac{\partial G}{\partial \mathcal{X}}(P_\varepsilon, Q) - \phi(Q) \frac{\partial^2 G}{\partial \mathcal{X} \partial \mathbf{n}}(P_\varepsilon, Q) \right) d\Gamma_Q d\Gamma_P \end{aligned} \quad (35)$$

Clearly any non-singular integral is continuous crossing the boundary and vanishes in the difference of the limits, leaving just the consideration of coincident and adjacent integrals. To see that the adjacent integrals can also be bypassed, first note that in this case the only contribution is from the hypersingular $\phi(Q)$ integral. The polar co-ordinate transformation establishes that the adjacent integral of the first derivative kernel is integrable for $\varepsilon=0$, hence continuous at the boundary, and thus must vanish. Similarly, for the hypersingular kernel, the only non-zero contributions must come at the common (singular) node: integrals involving shape functions that are zero at the common node are likewise well defined for $\varepsilon=0$ and must vanish. Thus, if $\phi(P_k)$ happens to be zero, the adjacent integral does not contribute to the gradient integral for this node. However, $\phi(P_k)=0$ can always be arranged: if the potential is shifted by a constant it remains a valid solution of the Laplace equation, and moreover, the gradient is unaltered. Therefore, in writing the gradient equation at P_k , all one has to do is to shift the potential by $-\phi(P_k)$, and the adjacent integral can be ignored.

4.2. Coincident integration

Let the element E for the coincident integral be defined by the two nodes $P_1 = (r_1, z_1)$ and $P_2 = (r_2, z_2)$, and define $c_r = r_2 - r_1$, $c_z = z_2 - z_1$ and $c^2 = c_r^2 + c_z^2$.

Although the expressions for the kernel functions are complicated, for gradient evaluation they become very simple. We begin by examining the integral of the flux, and from Equation (32) we obtain

$$r \hat{r} \frac{\partial G}{\partial \hat{r}} = \frac{1}{\pi} \frac{r \hat{r}}{2\hat{r}(a+b)^{1/2}} \left[\left(1 + \frac{2r\Delta r}{a-b} \right) E(m) - K(m) \right] \rightarrow \frac{1}{\pi} \frac{r \Delta r}{2(a-b)} \quad (36)$$

the arrow signifying the result of ignoring any term that is not sufficiently singular to survive the difference of the limits. Note that at the singular point $(\Delta r, \Delta z) \rightarrow 0$, and thus $\sqrt{a+b} \rightarrow 2\hat{z}$. In a similar fashion, for the derivative with respect to \hat{z}

$$r\hat{r} \frac{\partial G}{\partial \hat{z}} \rightarrow \frac{1}{\pi} \frac{r\Delta z}{2(a-b)} \quad (37)$$

For the gradient equation at P_k , the contribution from the flux integral is therefore $\partial\phi/\partial\mathbf{n}(P_j)\mathcal{J}_{kj}^{\mathcal{X}}$, where

$$\mathcal{J}_{kj}^{\mathcal{X}} = \left\{ \lim_{\varepsilon \rightarrow 0^-} - \lim_{\varepsilon \rightarrow 0^+} \right\} \frac{1}{\pi} \int_E \int_E \psi_k(P) \psi_j(Q) \frac{r\Delta\mathcal{X}}{2(\Delta r^2 + \Delta z^2)} d\Gamma_Q d\Gamma_P \quad (38)$$

where $k, j = 1, 2$ and once again \mathcal{X} is either \hat{r} or \hat{z} . These integrals can be computed analytically, and for the derivative with respect to \hat{r}

$$\begin{aligned} \mathcal{J}_{11}^{\hat{r}} &= c_z(3r_1 + r_2)/12, & \mathcal{J}_{12}^{\hat{r}} &= c_z(r_1 + r_2)/12 \\ \mathcal{J}_{21}^{\hat{r}} &= c_z(r_1 + r_2)/12, & \mathcal{J}_{22}^{\hat{r}} &= c_z(r_1 + 3r_2)/12 \end{aligned} \quad (39)$$

and for \hat{z}

$$\begin{aligned} \mathcal{J}_{11}^{\hat{z}} &= -c_r(3r_1 + r_2)/12, & \mathcal{J}_{12}^{\hat{z}} &= -c_r(r_1 + r_2)/12 \\ \mathcal{J}_{21}^{\hat{z}} &= -c_r(r_1 + r_2)/12, & \mathcal{J}_{22}^{\hat{z}} &= -c_r(r_1 + 3r_2)/12 \end{aligned} \quad (40)$$

The ‘simplification’ of the hypersingular integral, i.e. ignoring all non-singular terms, proceeds as above, with one change. In this case the order of the singularity is -2 , and the substitution $\sqrt{a+b} \rightarrow 2\hat{r}$ is no longer appropriate. The appropriate expansion in this case is

$$\begin{aligned} \frac{1}{(a+b)^{1/2}} &\approx \frac{1}{r+\hat{r}} = \frac{1}{2\hat{r}} + \left(\frac{1}{r+\hat{r}} - \frac{\Delta r}{2\hat{r}(r+\hat{r})} \right) \\ &= \frac{1}{2\hat{r}} - \frac{\Delta r}{2\hat{r}} \left(\frac{1}{2\hat{r}} + \left(\frac{1}{r+\hat{r}} - \frac{\Delta r}{2\hat{r}(r+\hat{r})} \right) \right) \approx \frac{1}{2\hat{r}} - \frac{\Delta r}{4\hat{r}^2} \end{aligned} \quad (41)$$

For the hypersingular kernels we therefore obtain

$$\begin{aligned} r\hat{r} \frac{\partial^2 G}{\partial \hat{r} \partial \mathbf{n}} &= \frac{1}{4\pi} \left[\frac{n_z \Delta z}{(\Delta r^2 + \Delta z^2)} + (r + \hat{r}) \left(\frac{n_r}{\Delta r^2 + \Delta z^2} - 2 \frac{\mathbf{n} \cdot \mathbf{R} \Delta r}{(\Delta r^2 + \Delta z^2)^2} \right) \right] \\ r\hat{r} \frac{\partial^2 G}{\partial \hat{z} \partial \mathbf{n}} &= \frac{1}{4\pi} \left[-\frac{n_r \Delta z}{(\Delta r^2 + \Delta z^2)} + (r + \hat{r}) \left(\frac{n_z}{\Delta r^2 + \Delta z^2} - 2 \frac{\mathbf{n} \cdot \mathbf{R} \Delta z}{(\Delta r^2 + \Delta z^2)^2} \right) \right] \end{aligned} \quad (42)$$

Note that with the additional \hat{r} factor from the weight function, these kernel functions present no problem at the axis. Moreover, it is expected (though we have not pursued this here) that a Galerkin treatment of the hypersingular flux equation (necessitating the use of the complete kernel functions), would also be without difficulty.

The integrals corresponding to Equation (38) are

$$\mathcal{J}_{kj}^{\mathcal{X}} = \left\{ \lim_{\varepsilon \rightarrow 0^-} - \lim_{\varepsilon \rightarrow 0^+} \right\} \int_E \int_E \psi_k(P) \psi_j(Q) r \hat{r} \frac{\partial^2 G}{\partial \mathcal{X} \partial \mathbf{n}} d\Gamma_Q d\Gamma_P \quad (43)$$

and analytic evaluation of the hypersingular integrals yields, for \hat{r} derivatives

$$\begin{aligned} \mathcal{J}_{11}^{\hat{r}} &= (c_r^2 + 3r_1c_r)/(6c), & \mathcal{J}_{12}^{\hat{r}} &= (-3r_1c_r - 3r_2c_r + c_r^2)/(12c) \\ \mathcal{J}_{21}^{\hat{r}} &= (3r_2c_r + 3r_1c_r + c_r^2)/(12c), & \mathcal{J}_{22}^{\hat{r}} &= (-3r_2c_r + c_r^2)/(6c) \end{aligned} \quad (44)$$

and for \hat{z}

$$\begin{aligned} \mathcal{J}_{11}^{\hat{z}} &= c_z(c_r + 3r_1)/(6c), & \mathcal{J}_{12}^{\hat{z}} &= c_z(c_r - 3r_1 - 3r_2)/(12c) \\ \mathcal{J}_{21}^{\hat{z}} &= c_z(c_r + 3r_2 + 3r_1)/(12c), & \mathcal{J}_{22}^{\hat{z}} &= c_z(c_r - 3r_2)/(6c) \end{aligned} \quad (45)$$

The simplified kernel expressions for gradient evaluation should be especially useful for axisymmetric elasticity, where the kernel functions are significantly more complicated [5, 7, 14].

5. NUMERICAL RESULTS

As a check on the above methods, the results of some simple numerical tests are presented below. In the first problem, the two-dimensional geometry is a circle of radius one centred at (2, 0), thus a torus in three dimensions. This problem is therefore simple in that any possible difficulties near the axis are avoided. The Dirichlet boundary condition is the harmonic function $\phi = x^2 + y^2 - 2z^2 = r^2 - 2z^2$, and the computed flux and post-processed surface gradient are compared with the easily obtained exact solutions. Listed in Table I are the discretized \mathcal{L}^2 errors

$$\left[\frac{1}{N} \sum_{j=1}^N (f_c(n_j) - f_x(n_j))^2 \right]^{1/2} \quad (46)$$

where f_c and f_x are the computed and exact values at the nodes n_j .

Two things should be noted. First, the convergence is approximately quadratic, which is the expected behaviour when using linear elements. Second, there is no point in proceeding too much further in the refinement of the boundary. As the interpolation and integration errors decay, eventually the approximation of the Green's functions via Equation (7), must begin to be a significant component of the error in the solution (as noted previously, the pointwise error in the four term expansions in Equation (7) is $< 2 \times 10^{-8}$). It can therefore be expected that the quadratic convergence with mesh size eventually disappears.

To test the axis treatment, the second example is the unit sphere, the two-dimensional geometry being $r^2 + z^2 = 1$, $r \geq 0$. Two different boundary conditions were employed, the first a point source located on the symmetry axis outside the sphere at (0.0, 1.2)

$$\phi = \frac{1}{(r^2 + (z - z_p)^2)^{1/2}} \quad (47)$$

The second used the same quadratic Dirichlet boundary conditions as above. The results are shown, respectively, in Tables II and III.

AXISYMMETRIC GALERKIN

Table I. \mathcal{L}^2 errors for the Dirichlet problem on the torus.

Elements	Flux	\hat{r} derivative	\hat{z} derivative
50	0.337E - 02	0.649E - 02	0.737E - 02
100	0.847E - 03	0.161E - 02	0.183E - 02
150	0.377E - 03	0.715E - 03	0.812E - 03
200	0.213E - 03	0.402E - 03	0.457E - 03
250	0.137E - 03	0.257E - 03	0.292E - 03
300	0.961E - 04	0.178E - 03	0.202E - 03
350	0.714E - 04	0.131E - 03	0.148E - 03
400	0.556E - 04	0.100E - 03	0.113E - 03
450	0.450E - 04	0.790E - 04	0.893E - 04

Table II. \mathcal{L}^2 errors for the Dirichlet problem on the sphere, with a point source located at (0, 1.2).

Elements	Flux	\hat{r} derivative	\hat{z} derivative
50	0.120E - 00	0.122E - 00	0.151E - 00
100	0.435E - 01	0.108E - 01	0.497E - 01
150	0.235E - 01	0.285E - 02	0.258E - 01
200	0.154E - 01	0.121E - 02	0.165E - 01
250	0.112E - 01	0.655E - 03	0.118E - 01
300	0.878E - 02	0.414E - 03	0.919E - 02
350	0.728E - 02	0.288E - 03	0.756E - 02
400	0.632E - 02	0.215E - 03	0.652E - 02

Table III. \mathcal{L}^2 errors for the Dirichlet problem on the sphere.

Elements	Flux	\hat{r} derivative	\hat{z} derivative
50	0.238E - 02	0.998E - 03	0.412E - 02
100	0.917E - 03	0.248E - 03	0.125E - 02
150	0.541E - 03	0.110E - 03	0.662E - 03
200	0.394E - 03	0.627E - 04	0.452E - 03
250	0.330E - 03	0.410E - 04	0.362E - 03
300	0.307E - 03	0.297E - 04	0.327E - 03
350	0.280E - 03	0.221E - 04	0.293E - 03
400	0.280E - 03	0.178E - 04	0.228E - 03

The convergence rate is clearly not as good as for the torus. An important aspect of the accuracy in the sphere tests is that, while the near-axis solution is reasonably accurate, nevertheless most of the error occurs in this region. For example, the pointwise error, as a function of θ , $0 < \theta < \pi/2$ ($\theta < 0$ is similar), for the quadratic boundary conditions with 200 elements, is plotted in Figure 2. Note that while the relative error at the axis ($\theta = \pi/2$) is quite acceptable, namely less than 0.1%, it is roughly two orders of magnitude larger than everywhere else.

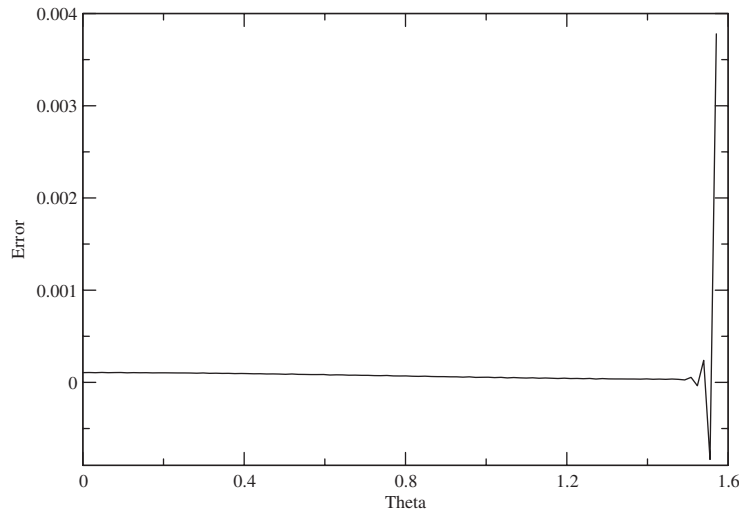


Figure 2. Pointwise error for the sphere problem, $0 < \theta < \pi/2$, with $\pi/2$ being the axis point.

One possible explanation for this might be that the integrations near the axis are not as accurate as elsewhere, though two diagnostics—the symmetry in the flux integral, and the row sums (which should be zero) for the potential integral—indicate that the axis integrations are just as accurate as other parts of the boundary.

The most likely source of the error at the axis is that the axial symmetry implies a smooth (zero derivative) solution at the axis, and the linear interpolation clearly violates this. As a test, the solution for a cylinder, $0 < r < 1$, $0.5 < z < 0.5$ was computed. The mixed boundary conditions were $\partial\phi/\partial\mathbf{n} = -1$ on $z = -0.5$, $\partial\phi/\partial\mathbf{n} = 0$ on $r = 1.0$, and $\phi = 1$ on $z = 0.5$. The solution is therefore linear, and this eliminates geometry and function interpolation errors at the axis, leaving (ignoring the very small errors introduced by the linear algebra solution) just errors in integration and the approximations of the elliptic integrals.

Figure 3 plots the error in potential on the bottom of the cylinder $y = -0.5$, and as can be seen, the axis solution, $r = 0$, is now just as accurate as the remainder of the geometry. Moreover, the solution for the flux on the top of the cylinder was virtually exact, and the errors are close to the level of accuracy in computing the elliptic functions. This would indicate that an appropriate interpolation at the axis is important, and obtaining an axis solution on par with the remainder of the geometry requires a higher order interpolation.

A final possibility is of course that there is an error in the code. However, as discussed above, the only difference between an axis and a non-axis point is the handling of the $\log(a+b)$ term in the coincident integration for an axis element. This part of the code appears to be implemented correctly.

As a final example, results are presented for two ‘sideways L-shaped’ domains, as illustrated in Figure 4. The motivation for considering this problem is that one of the intended applications of this work is to model (axisymmetric) drop dynamics [32] using a coupled boundary integral and Level Set [33] method. If an initial drop is to split into two, it will necessarily ‘pinch down’ near the axis, and thus a section of the boundary will run parallel and close to the

AXISYMMETRIC GALERKIN

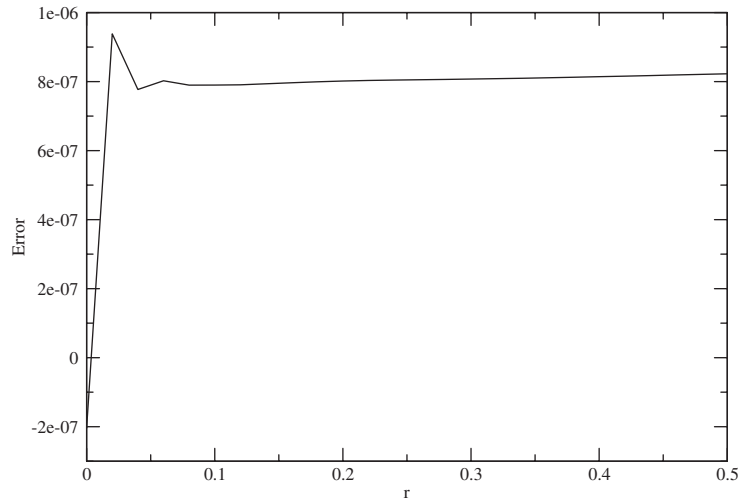


Figure 3. Pointwise error for the computed potential for the cylinder problem, $r=0$ being the axis point on the bottom of the cylinder.

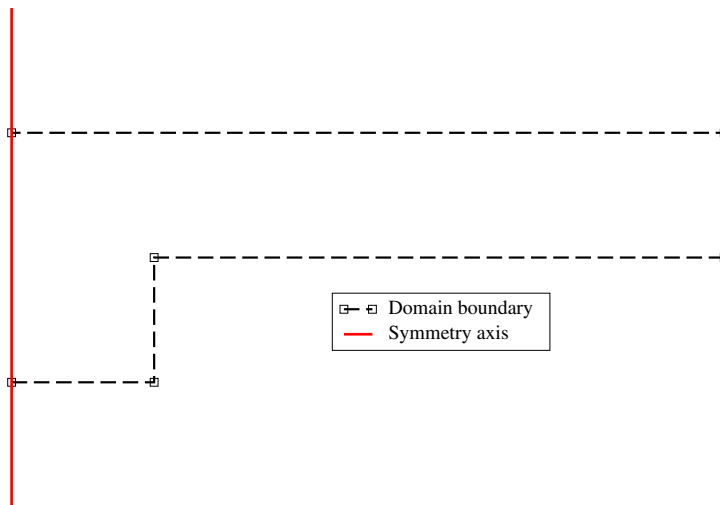


Figure 4. Sideways L-shaped domain.

symmetry axis. As the special form of the singularity at the axis may come into play here, the goal is to test the performance of the algorithm under these circumstances.

For the first geometry the vertices are $(0.0, -0.5)$, $(0.1, -0.5)$, $(0.1, 0.0)$, $(0.5, 0.0)$, $(0.5, 0.5)$, and $(0.0, 0.5)$, so that the distance to the axis along the lower vertical segment is 0.1. For the second geometry this distance is reduced to 0.05. We again apply the Dirichlet boundary

Table IV. \mathcal{L}^2 errors for the Dirichlet problem on the L-shaped domain. The distance to the symmetry axis in the first set is 0.1, and is 0.05 for the second set.

h	Flux	\hat{r} derivative	\hat{z} derivative
0.1667E-01	0.7710E-02	0.5732E-02	0.6527E-02
0.1000E-01	0.3621E-02	0.2701E-02	0.3054E-02
0.7143E-02	0.2310E-02	0.1722E-02	0.1913E-02
0.5000E-02	0.1876E-02	0.1369E-02	0.1445E-02
0.1250E-01	0.5052E-02	0.3747E-02	0.4281E-02
0.8333E-02	0.2785E-02	0.2080E-02	0.2338E-02
0.6250E-02	0.1933E-02	0.1443E-02	0.1587E-02

conditions $\phi = r^2 - 2z^2$, and thus at the corners there are two independent flux values to be determined. The Galerkin procedure allows for this, having two separate weight functions at the corner [34], but it is known that the errors at these Dirichlet corners is generally larger than at smooth boundary points. This is indeed what is seen in the calculated errors. The \mathcal{L}^2 errors, for several choices for mesh size h are given in Table IV. These numbers mostly reflect the flux errors at the corners, and the quadratic convergence is clearly lost. The errors in the middle of the segments are roughly one to two orders of magnitude less than at the corners. In particular, the errors are quite small along the vertical segment parallel and close to the symmetry axis.

6. CONCLUSIONS

A Galerkin boundary integral formulation for 3D axisymmetric problems has been presented. A primary feature of this approach is the use of modified weight functions, allowing a simplified treatment of the axis singularity, while restoring the symmetry present in other boundary integral formulations. As a consequence, a special axis treatment is not required: elements at the symmetry axis are handled, with the exception of one logarithm term, the same as any other element.

It was observed that, for curved geometries, the accuracy of the solution near the axis lagged behind that of the remainder of the boundary. The numerical tests appear to indicate that the fault lies with the linear interpolation, and a higher order approximation is required. This is currently being investigated.

Although we have only considered the axisymmetric Laplace equation, it is expected that the techniques will apply directly for the significantly more complicated situation present in axisymmetric elasticity. In particular, the double integral approach for handling the singular logarithm integrals is expected to result in a *relatively* simple implementation for the matrix kernel functions. Similarly, the Green's function quantities for the hypersingular traction equation are exceedingly lengthy, and the surface gradient algorithm presented herein should greatly simplify the evaluation of surface stress.

APPENDIX

Using the double integral approach, Equations (21) and (22), the logarithm integrals from the elliptic function approximations (Equation (25)) require the evaluation of

$$\int \frac{Z^j}{(Z^2 + \alpha^2)^{k+1/2}} dZ$$

$0 < k < 4$ and $0 < j < 2k + 2$. For those cases wherein the simple formulas are not finite at $\alpha = 0$, new expressions, derived as in Section 3.4.1, are presented below. These expressions unfortunately become somewhat lengthy for larger values of k , and we present them in a computationally convenient Horner form. Defining

$$\mathcal{P} = (Z^2 + \alpha^2)^{1/2}$$

we have

$$\int \frac{1}{(Z^2 + \alpha^2)^{3/2}} dZ = -\frac{1}{\mathcal{P}(Z + \mathcal{P})}$$

$$\int \frac{1}{(Z^2 + \alpha^2)^{5/2}} dZ = -3 \frac{3Z^2 + 4\alpha^2}{\mathcal{P}^3(3\alpha^2 Z + 2Z^3 + 2\mathcal{P}^3)}$$

$$\int \frac{Z^2}{(Z^2 + \alpha^2)^{5/2}} dZ = -3 \frac{3Z^4 + (3Z^2 + \alpha^2)\alpha^2}{\mathcal{P}^3(Z^3 + \mathcal{P}^3)}$$

$$\int \frac{1}{(Z^2 + \alpha^2)^{7/2}} dZ = -\frac{40Z^4 + (95Z^2 + 64\alpha^2)\alpha^2}{15\mathcal{P}^5(15\alpha^4 Z + 20\alpha^2 Z^3 + 8Z^5 + 8\mathcal{P}^5)}$$

$$\int \frac{Z^2}{(Z^2 + \alpha^2)^{7/2}} dZ = -\frac{15Z^6 + (40Z^4 + (20Z^2 + 4\alpha^2)\alpha^2)\alpha^2}{15\mathcal{P}^5(5\alpha^2 Z^3 + 2Z^5 + 2\mathcal{P}^5)}$$

$$\int \frac{Z^4}{(Z^2 + \alpha^2)^{7/2}} dZ = -\frac{5Z^8 + (10Z^6 + (10Z^4 + (5Z^2 + \alpha^2)\alpha^2)\alpha^2)\alpha^2}{5\mathcal{P}^5(Z^5 + \mathcal{P}^5)}$$

$$\int \frac{1}{(Z^2 + \alpha^2)^{9/2}} dZ = -\frac{140Z^6 + (476Z^4 + (567Z^2 + 256\alpha^2)\alpha^2)\alpha^2}{35\mathcal{P}^7(35\alpha^6 Z + 70\alpha^4 Z^3 + 56\alpha^2 Z^5 + 16Z^7 + 16\mathcal{P}^7)}$$

$$\int \frac{Z^2}{(Z^2 + \alpha^2)^{9/2}} dZ = -\frac{280Z^8 + (1015Z^6 + (1344Z^4 + (448Z^2 + 64\alpha^2)\alpha^2)\alpha^2)\alpha^2}{105\mathcal{P}^7(35\alpha^4 Z^3 + 28\alpha^2 Z^5 + 8Z^7 + 8\mathcal{P}^7)}$$

$$\int \frac{Z^4}{(Z^2 + \alpha^2)^{9/2}} dZ = -\frac{35Z^{10} + (140Z^8 + (140Z^6 + (84Z^4 + (28Z^2 + 4\alpha^2)\alpha^2)\alpha^2)\alpha^2)\alpha^2}{35\mathcal{P}^7(7\alpha^2 Z^5 + 2Z^7 + 2\mathcal{P}^7)}$$

$$\int \frac{Z^6}{(Z^2 + \alpha^2)^{9/2}} dZ = -\frac{7Z^{12} + (21Z^{10} + (35Z^8 + (35Z^6 + (21Z^4 + (7Z^2 + \alpha^2)\alpha^2)\alpha^2)\alpha^2)\alpha^2)\alpha^2}{7\mathcal{P}^7(Z^7 + \mathcal{P}^7)}$$

ACKNOWLEDGEMENTS

The authors gratefully acknowledge the support of the Spanish Ministry of Education, Culture and Sport through the Projects SAB 2003-0088 (LJG), and the Spanish Ministry of Science and Technology through Project MAT 2003-03315 (VM and EG). MG was supported by Spanish Project MEC-04-MTM-05417. LJG was also supported by the Applied Mathematical Sciences Research Program of the Office of Mathematical, Information, and Computational Sciences, U.S. Department of Energy, under Contract DE-AC05-00OR22725 with UT-Battelle, LLC. LJG would like to thank Prof. Federico Paris for the hospitality at the Escuela Superior de Ingenieros, Universidad de Sevilla, where this work was carried out.

The submitted manuscript has been authored by a contractor of the U.S. Government under Contract DE-AC05-00OR22725. Accordingly the U.S. Government retains a non-exclusive, royalty free license to publish or reproduce the published form of this contribution, or allow others to do so, for U.S. Government purposes.

REFERENCES

1. Cruse T, Snow DW, Wilson RB. Numerical solutions in axisymmetric elasticity. *Computers and Structures* 1977; **7**:445–451.
2. Kermandis T. A numerical solution for axially symmetric elasticity problems. *International Journal of Solids and Structures* 1975; **11**:493–500.
3. Mayr M. The numerical solution of axisymmetric elasticity problems using an integral equation approach. *Mechanics Research Communications* 1976; **3**:393–398.
4. Bakr AA. *The Boundary Integral Equation Method in Axisymmetric Stress Analysis*. Springer: Berlin, 1986.
5. de Lacerda LA, Wrobel LC. Hypersingular boundary integral equation for axisymmetric elasticity. *International Journal for Numerical Methods in Engineering* 2001; **52**:1337–1354.
6. de Lacerda LA, Wrobel LC. Dual boundary element method for axisymmetric crack analysis. *International Journal of Fracture* 2002; **113**:267–284.
7. Graciani E, Mantić V, Paris F, Blázquez A. Weak formulation of axi-symmetric frictionless contact problems with boundary elements. Application to interface cracks. *Computers and Structures* 2005; **83**:836–855.
8. Mukherjee S. Regularization of hypersingular boundary integral equations: a new approach for axisymmetric elasticity. *Engineering Analysis with Boundary Elements* 2002; **26**:839–844.
9. Bonnet M, Maier G, Polizzotto C. Symmetric Galerkin boundary element method. *Applied Mechanics Reviews* (ASME) 1998; **51**:669–704.
10. Danloy B. Numerical construction of Gaussian quadrature formulas for $\int_0^1 (-\log x)x^\alpha f(x) dx$ and $\int_0^\infty E_m(x)f(x) dx$. *Mathematics of Computation* 1973; **27**:861–869.
11. Zhao ZY, Lan S. Boundary stress calculation—a comparison study. *Computers and Structures* 1999; **71**:77–85.
12. Graciani E, Mantić V, Phan A, Gray LJ. Convergence studies for two boundary integral surface derivative methods, in preparation.
13. Gray LJ, Phan A-V, Kaplan T. Boundary integral evaluation of surface derivatives. *SIAM Journal on Scientific Computing* 2004; **26**:294–312.
14. Balaš J, Sládek J, Sládek V. *Stress Analysis by the Boundary Element Method*. Elsevier: Amsterdam, 1989.
15. Banerjee PK. *The Boundary Element Methods in Engineering*. McGraw-Hill: London, 1994.
16. Wrobel LC. The boundary element method. *Applications in Thermo-Fluids and Acoustics*, vol. I. Wiley: Chichester, 2002.
17. Liggett JA, Liu L-F. *The Boundary Integral Equation Method for Porous Media Flow*. Allen and Unwin: London, 1983.
18. Paris F, Cañas J. *Boundary Element Method: Fundamentals and Applications*. Oxford University Press: Oxford, 1997.
19. Gray LJ. Evaluation of singular and hypersingular Galerkin boundary integrals: direct limits and symbolic computation. In *Singular Integrals in the Boundary Element Method*, Sladek V, Sladek J (eds), Advances in Boundary Elements, Chapter 2. Computational Mechanics Publishers: Southampton, 1998; 33–84.
20. Milne-Thompson LM. Elliptic integrals. In *Handbook of Mathematical Functions*, Abramowitz M, Stegun IA (eds), Chapter 17. National Bureau of Standards: Washington, DC, 1972; 587–626.

AXISYMMETRIC GALERKIN

21. Whittaker ET, Watson GN. *A Course of Modern Analysis*. Cambridge University Press: Cambridge, MA, 2002.
22. Hastings C. *Approximations for Digital Computers*. Princeton University Press: Princeton, NJ, 1955.
23. Stroud A, Secrest D. *Gaussian Quadrature Formulas*. Prentice-Hall: Englewood Cliffs, NJ, 1966.
24. Crann D, Davies AJ, Christianson DB. Evaluation of logarithmic integrals in two-dimensional boundary element computation. In *Advances in Boundary Element Techniques IV*, Gallego R, Aliabadi MH (eds). Queen Mary University of London: London, U.K., 2003; 321–326.
25. Guiggiani M. Hypersingular formulation for boundary stress evaluation. *Engineering Analysis with Boundary Elements* 1994; **13**:169–179.
26. Okada H, Rajiyah H, Atluri SN. A novel displacement gradient boundary element method for elastic stress analysis with high accuracy. *Transactions of the ASME* 1988; **55**:786–794.
27. Schwab C, Wendland WL. On the extraction technique in boundary integral equations. *Mathematical Computation* 1999; **68**:91–122.
28. Wilde AJ, Aliabadi MH. Direct evaluation of boundary stresses in the 3D BEM of elastostatics. *Communications in Numerical Methods in Engineering* 1998; **14**:505–517.
29. Zhao Z. On the calculation of boundary stresses in boundary elements. *Engineering Analysis with Boundary Elements* 1997; **16**:317–322.
30. Graciani E, Mantič V, Paris F, Cañas J. A critical study of hypersingular and strongly singular boundary integral representations of potential gradient. *Computational Mechanics* 2000; **25**:542–559.
31. Mantič V, Graciani E, Paris F. A simple local smoothing scheme in strongly singular boundary integral representation of potential gradient. *Computer Methods in Applied Mechanics and Engineering* 1999; **178**:267–289.
32. Notz PK, Basaran OA. Dynamics of drop formation in an electric field. *Journal of Colloid and Interface Science* 1999; **213**:219–237.
33. Sethian JA. *Level Set Methods and Fast Marching Methods: Evolving Interfaces in Computational Geometry, Fluid Mechanics, Computer Vision, and Materials Science*. Cambridge University Press: Cambridge, MA, 1999.
34. de Paula FA, Telles JCF. A comparison between point collocation and Galerkin for stiffness matrices obtained by boundary elements. *Engineering Analysis with Boundary Elements* 1989; **6**:123–128.